2004

Design and Optimization of Capillary Tube-Suction Line Heat Exchangers

Gaurav Jain
University of Illinois at Urbana-Champaign

Clark Bullard
University of Illinois at Urbana-Champaign

DESIGN AND OPTIMIZATION OF CAPILLARY TUBE-SUCTION LINE HEAT EXCHANGERS

Jain, Gaurav[1], Bullard, Clark[2]
[1]Graduate Student, University of Illinois, Department of Nuclear Engineering, Urbana, Illinois
jain2@uiuc.edu Phone: 217-333-6899
[2]Research Professor, University of Illinois, Department of Mechanical Engineering, Urbana, Illinois
bullard@uiuc.edu Phone: 217-333-7734

ABSTRACT

The effect of capillary tube-suction line heat exchanger (ctslhx) geometry on system performance was explored at various design and off-design conditions by embedding it in a system model. A detailed finite-volume model of the capillary tube and suction line, capable of handling all the phase-change complexities was used. All the ctslhx configurations considered meet the design constraints and didn't affect the design COP very much. Captubes with large inlet sections and relatively small outlets were found to give best performance at all the simulated off-design perturbations.

1. INTRODUCTION

R134a vapor compression cycle efficiency benefits greatly from suction line heat exchange (Domanski *et al*., 1994). The capillary tube suction line heat exchanger in a domestic refrigerator/freezer consists of an adiabatic inlet section, a heat exchanger section and an adiabatic outlet section. The refrigerant exiting from the condenser flashes in the adiabatic inlet section and enters the heat exchanger section of the captube (Fig. 1), where it rejects heat to the cold suction line downstream of the evaporator and enters the adiabatic outlet section at reduced quality and pressure. It then exits at a choked condition and expands discontinuously to the evaporator (Moreira and Bullard, 2003).

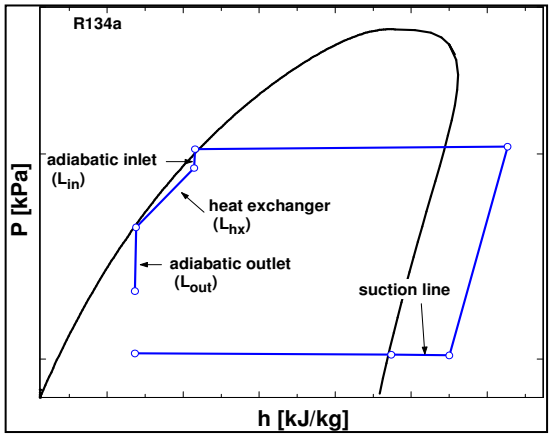

Figure 1: CTSLHX on a P-h diagram

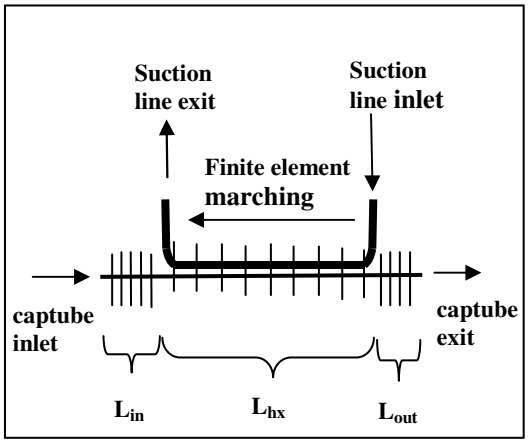

Figure 2: Division of elements in the captube model

The ctslhx dimensions play an important role in deciding its contribution to the system performance. Since the heat exchanger length is maximized to utilize whatever suction line length is accessible, it is important to identify what all combinations of captube diameter and inlet and outlet adiabatic lengths can give stable and efficient performance both at design and off-design conditions. This paper analyses the effect of capillary tube geometry on system performance by embedding it in a system simulation model. In the next section we briefly describe the modeling approach and assumptions made to model individual components. Section 3 presents the design point (standard 90°F

(32°C) ambient dry coil test condition (USDoE, 1988)) results where a large set of inlet and outlet lengths are considered. The critically charged system is then analyzed for stability and performance by allowing it to react to some off-design perturbations as explained in section 4. The paper ends with some conclusive remarks about the desirable and avoidable captube geometries for efficient and stable operation.

2. SIMULATION MODEL

A Newton-Raphson based solver, EES (Klein and Alvarado, 1995) was used to solve the pressure-enthalpy equations describing the interactions among all the system components including the cabinet. Each component was modeled using detailed equations in its own subroutine that was designed to solve sequentially, as described below. Refrigerant charge calculations were done for each component and summed to obtain the total charge in the system.

2.1 CTSLHX

A finite volume approach was used in the modeling of ctslhx because of highly nonlinear behavior and large pressure drops. Since the inlet and outlet lengths are just adiabatic capillary tubes, a single routine was used to handle both of them. A separate routine was, however required for the heat exchanger section to model the simultaneous heat transfer and pressure drop taking place in it. The ctslhx was solved by marching upstream on the captube side and downstream on the suction side (Fig. 2). As a result a sequential run required critical conditions at the captube exit and inlet conditions for the suction line.

Equilibrium equations were used throughout, recognizing that they slightly underestimate mass flow rate in adiabatic (Meyer and Dunn, 1996) and diabatic (Liu and Bullard, 2000) capillary tubes. Since correction factors are not well developed for R134a, they can be neglected here in the interest of providing insights into ctslhx behavior by exploring the parameter space using physically-based equations.

2.1.1 Adiabatic section: The whole of the adiabatic length was divided into a number of equally sized finite elements. The routine was capable of handling both the single and two-phase regions and any transitions (flashing, re-condensation). Following Bittle and Pate (1996) the fiction of a two-phase viscosity was employed to model the frictional pressure drop (Eq. 1). Calculating the critical mass flux (Eq. 2) at the choked homogeneous isentropic captube exit was the first step in the sequential solution. Equilibrium equations were used for the calculation of two-phase acceleration pressure drop.

$$\frac{1}{\mu_{2\phi}} = \frac{1-x}{\mu_l} + \frac{x}{\mu_v} \tag{1}$$

$$G_{crit} = \rho \sqrt{\left(\frac{\partial P}{\partial \rho}\right)_s} \tag{2}$$

2.1.2 Heat exchanger section: Each element of the heat exchanger section was modeled as a simple tube-by-tube counterflow heat exchanger. Within each finite element fluid properties were assumed constant and suction side pressure drop was calculated after the heat transfer was determined. Since the pressured drop was large in a cap-tube element, it was calculated simultaneously with the heat transfer. The methodology for the calculation of pressure drop in the heat exchanger part of the captube was same as that for the adiabatic part. The suction line pressure was adjusted for pressure drop by using Churchill (1997) correlation for single phase and Souza and Pimenta (1995) correlation for two-phase. The acceleration pressure drop and the fluid kinetic energy were neglected in the heat exchanger section because it is small, but treated explicitly in the adiabatic sections where it can be quite large.

The heat transfer from the captube to the suction line was calculated using ε-NTU relations (Incropera & DeWitt, 1996). Because of high pressure drop, the two-phase temperature in the captube was taken to be the average value of the element inlet and outlet temperatures. Single phase heat transfer coefficient was obtained using Gnielinski (1976) correlation for both the captube and the suction side. The correlations from Dobson and Chato (1998) provided the two-phase heat transfer coefficient for the captube side, and Wattelet *et al*. (1994) for the suction side. When flashing or recondensation occurred within an element, it was split into two sub-elements that were solved

separately. The model was well equipped with different routines to handle subcooled and two-phase refrigerant on the captube side and two-phase and superheated refrigerant on the suction side, along with any phase changes.

2.2 Evaporator and Condenser

The evaporator model simulated a typical finned tube design used in auto-defrost refrigerators. A single tube circuit serpentines downwards from the refrigerant inlet to the air inlet, and then serpentines upward to join the suction line. The downward tube passes were modeled as an overall counterflow heat exchanger and the upward passes as an overall parallel flow; each seeing half the evaporator air flow. The condenser was a cross-counterflow wire-on-tube type condenser, consisting of 15 rows in the air flow direction with two passes per row. A multi-zone approach was used to solve both the components. Depending upon the refrigerant state, the evaporator was divided into two-phase and superheated parts and the condenser into subcooled, two-phase and superheated zones. Heat transfer in each zone was calculated by using ε-NTU relations. Correlations from Wattelet *et al.* (1994) (evaporation), Dobson and Chato (1998) (condensation) and Gneilinski (1976) (single phase) were used to obtain refrigerant side heat transfer coefficient. Wang and Chang (2000) correlation provided the air side heat transfer coefficient for the evaporator. The same was obtained for the condenser from Hoke *et al*. (1997), as modified by Petroski and Clausing (1999).

The compressor was modeled using standard 10-parameter polynomial curve fits provided by the manufacturer, expressing mass flow rate and power as function of suction and discharge pressures. A scaling factor was used to size the compressor to meet the load at the target runtime at the design condition.

3. TRADEOFFS AT THE DESIGN CONDITION

The model was run in design mode for a fixed superheat and subcooling of 2°C at 90°F (32°C) ambient temperature. The compressor was sized for a run time fraction 0.6 at the design condition. Over the wide range of captube adiabatic inlet and outlet lengths considered, (0.524m < L_{in} < 2.024m and 0.3m < L_{out} < 2.0m), each combination required a slightly different captube diameter, compressor size and total system charge.

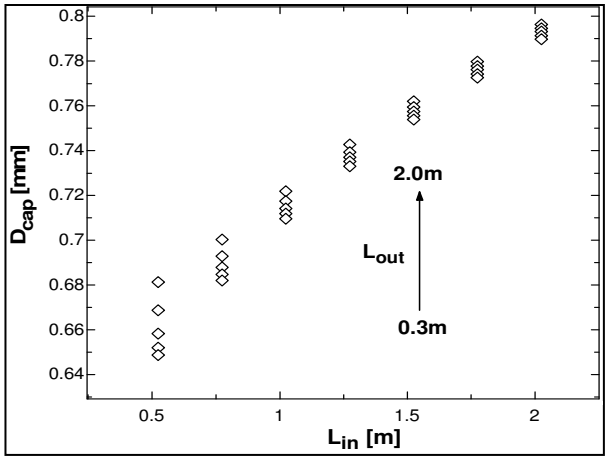

Figure 3: Dependence of captube diameter on inlet and outlet length

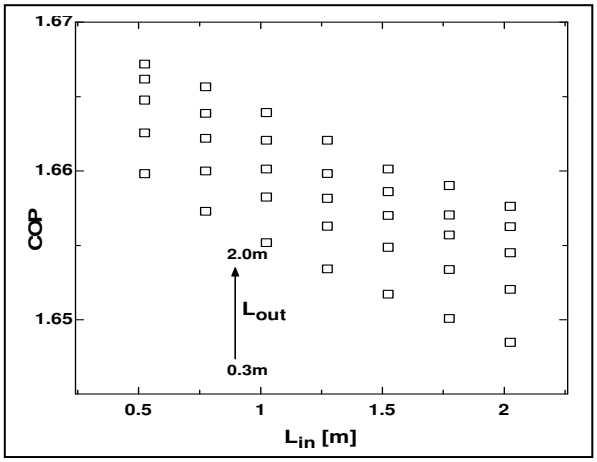

Figure 4: Variation of system COP with inlet and outlet length

Generally, longer captubes require a larger diameter to carry the design mass flow rate, as shown in Fig. 3. Increasing inlet length creates more two-phase pressure drop and therefore a lower temperature at the inlet of the heat exchanger section. This diminishes heat transfer from the captube and hence increases evaporator inlet enthalpy, thus requiring an increased mass flow rate to satisfy the design load. The extra pressure drop in the inlet section forces the captube's choked exit to occur at lower pressures, where density is lower. Hence it requires an increased diameter to carry this extra mass flow rate. On the other hand, the captube diameter is only slightly dependent on the outlet length. For a particular inlet length, a long outlet section generates more pressure drop causing the refrigerant to exit at lower density, so the diameter must increase to carry this high volume fluid. Now since the tube is fatter, there is slightly less pressure drop in the inlet section and hence slightly more heat transfer

occurs. The resultant lower evaporator inlet enthalpy requires less mass flow rate to match the load. As a result the net increase in diameter is small.

Fig. 4 shows how design COP varies with L_{in} as outlet length increases from 0.3m to 2.0m. Surprisingly the effect on COP at the design condition is quite small. Smaller inlet lengths fetched a higher value of COP because smaller inlet pressure drop provides higher inlet temperature to the heat exchanger section. The larger heat transfer increases the refrigerating effect and hence the COP. The COP increases with outlet length, though the effect is much smaller. Thus at the design condition COP is maximized by selecting the longest outlet and shortest inlet length. By maximizing the refrigeration effect through internal heat exchange, the refrigerant mass flow rate is also minimized, so the most efficient system also requires smallest compressor. Note that the COP variation for all the configurations simulated is only 1.15% because the ctslhx is already operating at high effectiveness (~80%) as it is utilizing the maximum available suction line length.

4. OFF-DESIGN BEHAVIOR

After the captube geometry has been fixed at the design condition, it is important to see how it reacts to changes in external conditions such as weather, door openings, frosting and dust fouling. A complete system simulation would involve letting these variables change across their full operational range, while observing the performance of the system capacity and COP in general, and the CTSLHX inlet/outlet states in particular. The most important objective would be to prevent liquid from entering the compressor and to maintain adequate capacity at high ambient temperatures. To analyze the off-design behavior, nine combinations of L_{in} and L_{out} representative of the whole range of inlet and outlet lengths examined at the design point were selected. Table 1 shows the chosen 9 combinations and their performance at the design point, with S, M and L designating short, medium and long inlet/outlet sections, respectively. Four types of off-design conditions were simulated:

1) Letting the system react to a room temperature change across a wide range of 16°C to 49°C.
2) Increasing the evaporator air inlet temperature to 10°C to simulate frequent door openings and resultant high load conditions.
3) Reducing the evaporator air flow rate by half to account for excessive frosting.
4) Reducing the condenser air flow rate by half to account for dust fouling or blockage of the outdoor coil.

Table 1: Performance of ctslhx configurations at the design condition

Captube	L_{in} [m]	L_{out} [m]	COP	D_{cap} [mm]	$\dot{V}_{flow}$ [m^3/s]*1000
SS	0.524	0.3	1.660	0.649	0.2345
SM	0.524	1.0	1.664	0.655	0.2343
SL	0.524	2.0	1.667	0.681	0.2339
MS	1.024	0.3	1.655	0.710	0.2352
MM	1.024	1.0	1.659	0.713	0.2348
ML	1.024	2.0	1.664	0.722	0.2342
LS	2.024	0.3	1.648	0.790	0.2363
LM	2.024	1.0	1.653	0.792	0.2357
LL	2.024	2.0	1.658	0.796	0.2348

4.1 Ambient temperature

Figure 5 shows how COP of systems having the above nine ctslhx configurations would change with the ambient temperature. As we move off-design by increasing the ambient temperature the COP decreases and remains pretty close for all the cases. As the evaporator exit becomes saturated due to increased refrigerant flow, heat exchanger protects the compressor inlet by maintaining superheat. As ambient temperature falls below the design point, COP increases due to a decrease in compressor work requirement. But this increase in COP is not alike for all the cases and gets hindered after some point. For a particular inlet length, the poor-performing captubes were identified as those having relatively long outlet sections. A marked difference of 9% can be seen in the COP of systems SS and SL at 21°C (a more common operating condition).

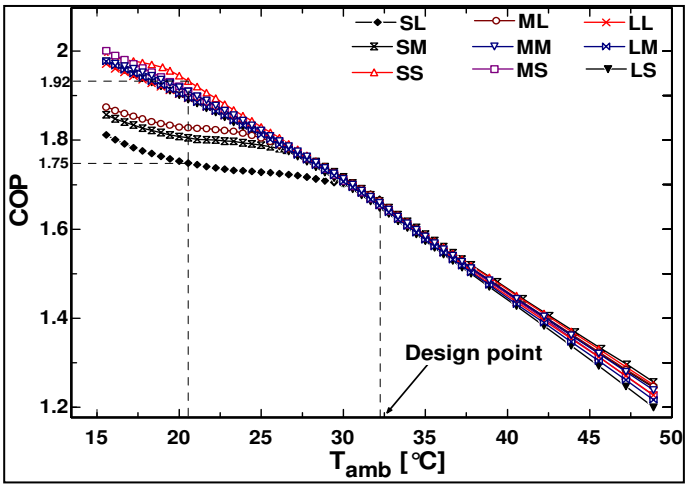

Figure5: Variation of COP with the ambient temperature

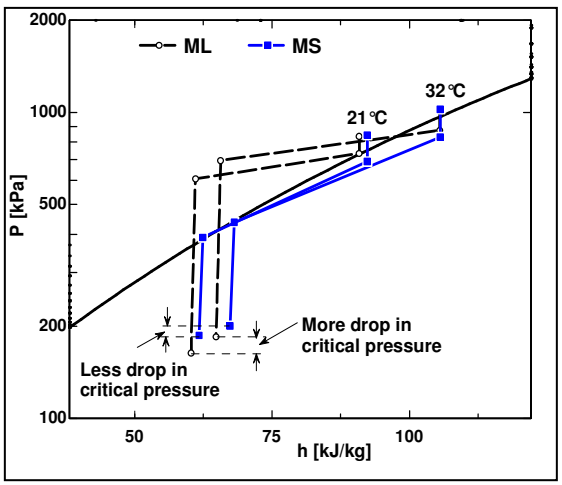

Figure 6: Inlet and outlet states of captubes ML and MS at 32 and 21°C ambients

To explain this behavior we consider two captubes; MS and ML. Both of them have same inlet length (1.024m) but different outlet lengths (0.3m and 2.0m respectively). At 21°C MS has about 3.7% greater COP than ML. When the ambient temperature decreases, the captube inlet state moves down and to the left (Figure 6) and the captube reacts by moving its choked exit down and towards left, decreasing mass flow rate due to lower exit density. The compressor reacts by lowering T_{evap} to equalize the mass flow rate, increasing the size of the evaporator's superheated zone. The mass flow rate and T_{evap} reduction is far greater in the case of ML because its choked exit moves down faster (Figure 6). The system COP's soon diverge because the rapidly decreasing evaporating temperature increases the specific volume at the suction inlet, increasing the compressor work faster than the falling condensing temperature reduces it.

For all configurations, the run-time fraction (Q_{evap}/Q_{load}) reached unity somewhere around 47°C and was found insensitive to the individual captube dimensions. During all off-design perturbations in ambient temperature, the compressor received superheated vapor with all captube geometries. Hence, there was no threat to the compressor. The variation of COP with ambient temperature highlights the poor performance of captubes SM, SL and ML. Although these tubes which have large outlet length as compared to the inlet deliver slightly higher COP at the design point, their performance off-design is poor. Region 1 in Figure 11 shows badly performing captubes on an L_{out} vs. L_{in} plot. Due to their poor performance at low ambient temperatures, captubes SM, SL and ML will not be pursued in further analyses.

4.2 Evaporator and Condenser air flow rates

The system was subjected to variations in evaporator and condenser air flow rates at the more common operating condition of 21°C. The effect of decreasing condenser air flow rate on system performance can be seen in Figure 7. The volumetric air flow rate over the condenser coil was decreased from a design point value of $0.055m^3/s$ to $0.0275m^3/s$. The COP decreases because of decreasing face velocity and increase in LMTD caused by doubling the rise in air temperature. All the captubes showed similar trend in the COP and no marked difference in the performance was observed.

To simulate the effect of air flow blockage due to frosting in evaporator, the evaporator volumetric flow rate was decreased by half from its design point value of $0.021m^3/s$ to $0.011m^3/s$. Again the COP decreased (Fig. 8) due to reduction in face velocity and increase in LMTD. Again as in the case with condenser, all the captubes showed similar trend in the performance. The above simulation results suggest that changes in air flow rates affect system performance in ways that do not upset the balance between the compressor and ctslhx refrigerant flow rates, so the results are relatively insensitive to ctslhx configuration. The compressor was protected in all cases as the suction line remained superheated.

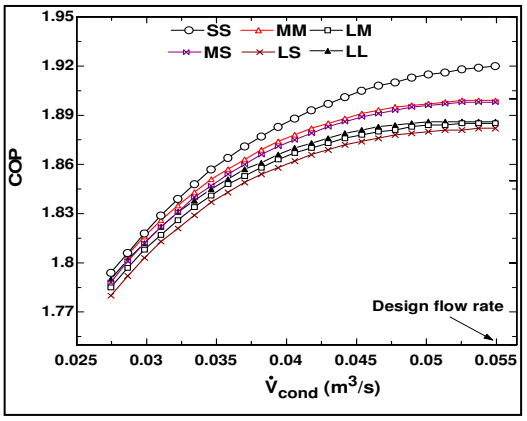

Figure 7: Condenser air flow degradation (T_{amb} = 21°C)

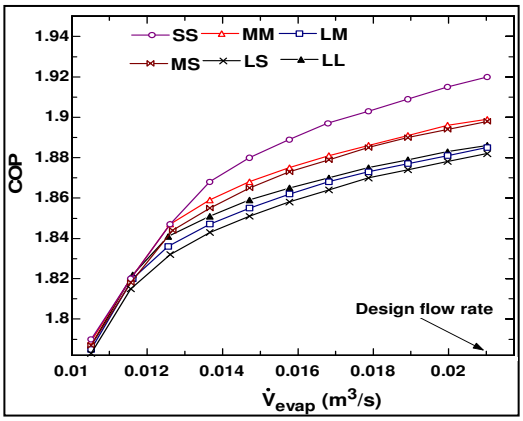

Figure 8: Evaporator air flow degradation (T_{amb} = 21°C)

4.3 Evaporator air inlet temperature

The evaporator air inlet temperature was varied from -12.8°C to 10°C to simulate the effect of frequent door openings at 21°C ambient. The COP firstly increases with the inlet temperature and then decreases (Fig. 9). It is seen that for captubes SS, MM and LL, the COP decreases sooner and faster as compared to captubes MS, LS and LM. A COP difference of about 5.5% was observed between tubes MS and MM at air inlet temperatures near 0°C. As the cabinet temperature increases, the evaporating temperature rises, thereby increasing the compressor's mass flow rate and consequently the condensing pressure. The captube accommodates this increased mass flow rate by raising its critical exit pressure and density. The increased superheat at the evaporator exit decreases the heat transfer in the captube, moving the critical point right in the P-h plane (Fig. 10). Captubes SS, MM and LL fail to accommodate the increasing mass flow rate demanded by the increasing load. As the evaporator is starved and its superheated region grows, the compressor mass flow rate adjusts and the suction pressure falls. This increases the suction specific volume and hence specific work. As a result a drop in COP is observed. Captubes MS, LS and LM are able to meet the increasing demand in mass flow rate and hence show an increase in the COP.

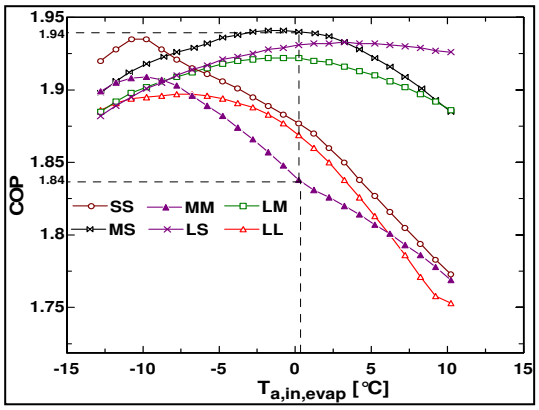

Figure 9: Variation of COP with evaporator air inlet temperature at 21°C

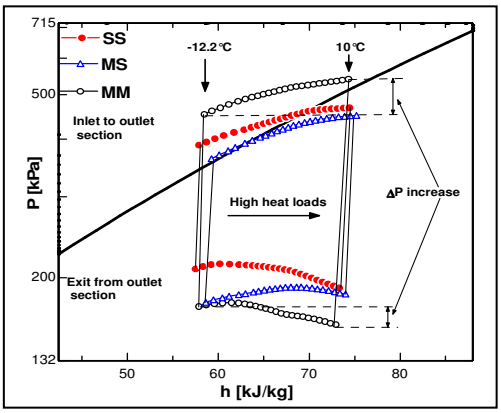

Figure 10: Movement of critical point with evaporator air inlet temperature at 21°C

The above observations can be explained by considering tubes SS, MS and MM and plotting the trajectories of inlet and outlet states of their adiabatic outlet section on a P-h diagram (Fig. 10). As load on the system increases, the increasing condensing temperature forces the inlet to the outlet adiabatic section up and towards the right. The critical exit temperature increases to carry the increased mass flow rate. But as the outlet section moves towards the right, a greater portion of it experiences two phase pressure drop (it increases from 5% to 65% for captube MM over the range of heat loads simulated). The resulting increase in the outlet section pressure drop and critical quality both tend to decrease the mass flow rate. These two effects compete with the increasing condensing temperature and soon overcome it. As a result the captube now exits at much lower critical pressure, where it can carry only less mass

flow rate due to lower density. This can be seen in Fig. 10 for tubes SS and MM. The above phenomenon is not so prominent with captube MS because initially 80% of its outlet length was two phase. The rightward movement of the vertical adiabatic line does not add to the two phase pressure drop greatly and hence this captube is able to meet the increased demand in the mass flow rate. As a result the COP increases. It was also noticed that the capacity decreases for captubes SS, MM and LL and increases for MS, LS and LM with the increase in heat load. Captube MS was found to deliver about 12% more COP than captube MM near 0°C. So the latter (more efficient) cap-tubes were able to provide the capacity when it was required most while the former ones failed to do so.

The simulations at high heat load perturbations revealed that it is desirable to have ctslhx configurations where refrigerant leaves the heat exchanger section inside or near the dome boundary. This can be achieved by having long inlet and short outlet lengths. The region of such desirable tubes is marked in Fig. 11.

5. RESULTS AND CONCLUSIONS

The simulations reported in this paper revealed that COP at the design condition could be held within 1.2% of its maximum value as ctslhx adiabatic inlet and outlet lengths varied over a wide range ($0.524m < L_{in} < 2.024m$ and $0.3m < L_{out} < 2.0m$). For each configuration, the required mass flow could be achieved through minor adjustments in captube diameter, compressor displacement, and charge. This gives engineers great flexibility to design the ctslhx without sacrificing more than 1% of design COP, at the standard test conditions, and to choose the combination of L_{in} and L_{out} that meet other performance objectives at off-design conditions.

A variety of off-design conditions were simulated to examine the effects of changing ambient temperature, frequent door openings, and excessive frosting, dust fouling and air flow blockage. All the combinations gave almost same performance with increasing ambient temperature. However at low ambient conditions, captubes with long outlet sections have much lower COP than other configurations due to high compressor work. System SL was found to be 9% less efficient than system SS at 21°C. The run-time fraction for all the captubes reached unity at about 47°C ambient. No marked difference was seen in the performance of the captubes with respect to changing evaporator and condensing air flow rates. For a given inlet length, captubes with small outlet lengths gave better performance than those having large outlet sections at higher evaporator air inlet temperatures. Captube MS was seen to have 5.5% higher COP and 12% higher capacity than captube MM at 0°C air inlet temperature. In all of the above off-design steady state conditions, the compressor received superheated vapor because the ctslhx was large enough to handle any excessive liquid.

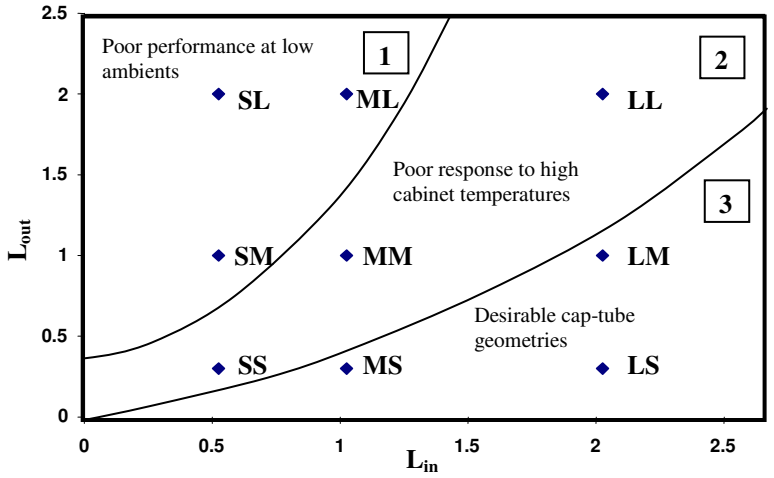

Figure 11: Regions identifying good and bad performing captube geometries

Since all the ctslhx configurations are able to meet the design constraints and perform equally at the design point, off-design conditions determine their selection. Those having large inlet and relatively short outlet give better and stable performance at all the tested off-design conditions because the inlet to the adiabatic outlet section remains close to the dome. Region 3 in Figure 11 identifies the most favorable parameter range. Factors like hot-weather capacity and maintaining compressor suction superheat are not an issue in the captube design. Finally, tolerances on

captube diameter, routing requirements for inlet and outlet segments and material costs may dictate the final selection of the captube geometry.

NOMENCLATURE

COP	coefficient of performance	(-)	**Subscript**	
D	diameter	(mm)	2ϕ	two-phase
G	refrigerant mass flux	(kg/m^3-s)	a	air
h	enthalpy	(kJ/kg)	cap	capillary tube
L_{in}	adiabatic inlet length	(m)	cond	condenser
L_{hx}	heat exchanger length	(m)	crit	critical conditions
L_{out}	adiabatic outlet length	(m)	evap	evaporator
μ	viscosity	(kg/m-s)	in	inlet
P	pressure	(kPa)	l	saturated liquid
Q_{evap}	evaporator capacity	(kW)	s	entropy
Q_{load}	heat load on the system	(kW)	v	saturated vapor
ρ	density	(kg/m^3)		
T	temperature	(°C)		
$\dot{V}_{flow}$	volumetric flow rate	(m^3/s)		

REFERENCES

AHAM, 1988, Household refrigerators/household freezers, *ANSI/AHAM STANDARD HRF-1-1988*, Chicago, IL.

Bittle, R.R., Pate, M.B., 1996, A theoretical model for predicting adiabatic capillary tube performance with alternative Refrigerants, *ASHRAE Transactions*, 102(2):52–64.

Churchill, S.W., 1997, Friction-factor equations spans all fluid flow regimes, *Chemical Engineering*, p. 91-92.

Dobson, M.K., Chato, J.C., 1998, Condensation in Smooth Horizontal Tubes, *Transactions of ASME, Journal of Heat Transfer*, 120, 193-213.

Domanski, P., Didion, D., Doyle., J., 1994, Evaluation of suction-line/liquid-line heat exchange in the refrigeration cycle, Int. J. Refrig.; 17(7):487-493.

Gnielinski V., 1976, New equations for heat and mass transfer in turbulent pipe and channel flow, *Int Chem Engg* 16, p. 359-368.

Hoke, J.L., Clausing, A.M., Swofford, T.D., 1997, An Experimental Investigation of Convective Heat Transfer from Wire-on-Tube Heat Exchangers, *ASME Journal of Heat Transfer*, 119, 3487-356.

Incropera FP., Dewitt DP., 1996, *Fundamentals of Heat and Mass Transfer 4th edition*, John Wiley & Sons, New York.

Klein, S., Alvarado, F., 1995, Engineering Equation Solver, F-Chart Software, Middletown, WI.

Liu, Y., Bullard, C.W., 2000, Diabatic Flow Instabilities in Capillary Tube-Suction Line Heat Exchangers, *ASHRAE Transactions*, 106:1, 517-523.

Meyer, J.J., W.E., Dunn, 1996, Alternative Refrigerants in Adiabatic Capillary Tubes, University of Illinois at Urbana-Champaign, ACRC TR-067.

Moreira, J.R., Bullard, C.W., 2003, Pressure drop and flashing mechanisms in refrigerant expansion devices, *Int. J. Refrig*., vol. 26, no. 7: p. 840-848

Petroski, S.J., A.M., Clausing, 1999, An Investigation of the Performance of Confined, Saw-Tooth Shaped Wire-on-Tube Condensers, University of Illinois at Urbana-Champaign, ACRC TR-153.

Souza, A., Pimenta, M., 1995, Prediction of pressure drop during horizontal two-phase flow of pure and mixed refrigerants, In: Katz J, Matsumoto Y, editors. Cavitation & Multiphase flow, New York (NY): ASME, FED-Vol. 219, p. 161-71.

Wang, C., Kuan-Yu, C., Chang C., 2000, Heat transfer and friction characteristics of plain fin-and-tube heat exchangers, *International Journal of Heat and Mass Transfer*, vol. 43 (2000), p. 2693-2700.

Wattelet J., Chato J., Souza A., Christofferson B., 1994, Evaporative Characteristics of R-12, R-134a and a Mixture at Low Mass Fluxes, ASHRAE Trans.;100(1):603-615.